Local-field effects and anisotropic plasmon dispersion in diamond

S. Waidmann, M. Knupfer, B. Arnold, and J. Fink

Institut für Festkörper- und Werkstofforschung Dresden, Postfach 270016, D-01171 Dresden, Germany

A. Fleszar and W. Hanke

Institut für Theoretische Physik I, Universität Würzburg, am Hubland, D-97074 Würzburg, Germany

(Received 1 December 1999)

We have measured the plasmon dispersion of diamond along the high-symmetry directions using electron energy-loss spectroscopy in transmission. We found the plasmon dispersion to be considerably anisotropic. A comparison of the experimental results to *ab initio* calculations that take local-field effects into account demonstrates the importance of local-field effects for the dielectric response of systems with strongly inhomogeneous electron distributions.

I. INTRODUCTION

Diamond is the model substance of a solid with pure covalent bonds. The carbon atoms are sp^3 hybridized, which means that every carbon atom has four nearest neighbors in a tetrahedral arrangement. Between the atoms there are pronounced bonds where the electrons are strongly localized. This leads to a considerably inhomogeneous electron distribution. Consequently, local-field effects play a significant role for a complete description of the electronic properties.[1,2] The importance of local-field effects for a complete understanding of systems exhibiting inhomogeneous charge distributions has long been realized and discussed for a number of materials including Si, Ge, and GaAs, which are also of technological potential.[3–12] Despite this effort, there is a general lack of experimental studies that are undispensable to decide which theoretical model is best suited to handle the local-field effects and to extract their consequences on various electronic properties.

A widespread method to determine the electronic/dielectric properties is optical spectroscopy. In crystals with cubic symmetry like diamond, the response in the optical limit is isotropic. The restriction in optics to momentum transfers nearly zero is a serious drawback of this method. It can be overcome by the use of electron energy-loss spectroscopy (EELS), where one measures the loss function Im $[-1/\epsilon(q,\omega)]$, i.e., the response of a system to a longitudinal perturbation, with the possibility to vary the momentum transfer independently. One thus has access to the dielectric response as a function of both energy and momentum. Moreover, as the wavelength of an excitation becomes smaller with increasing momentum,[13] one can tune the sensitivity of EELS to the local inhomogeneity of the electronic systems under consideration.

At longer wavelengths the loss function is dominated by collective excitations of the electron system, i.e., the plasmons.[14] Plasmons in nearly free electron systems, like simple metals, can be described in the framework of the self-consistent field method or random phase approximation (RPA). At long wavelengths also in semiconductors plasmons are the dominant excitations but, in this case, the band structure of the solid has to be taken into account.[15] If one has to deal with inhomogeneous electron systems, crystal local-field effects (CLFE), which are described by the off-

diagonal elements of the dielectric matrix $[\epsilon_{\mathbf{GG'}}(\mathbf{q},\omega)$, $\mathbf{G}=$ reciprocal lattice vector], additionally have to be considered.[16,17] This means that the polarization due to an external perturbation fluctuates on the atomic scale. With this the response of the system includes, in addition to the wavelength of the external perturbation $[\mathbf{E}(\mathbf{q},\omega)]$, electric fields with wavelengths of the order of lattice spacings, or in a Fourier description, Bragg diffracted components $[\mathbf{E}(\mathbf{q}+\mathbf{G},\omega)]$.[1] These effects should not be confused with many-particle ''local-field'' effects due to exchange and correlation (XCLFE). In the following, we explore the importance of both types of local-field effects for the longitudinal dielectric response of diamond.

Taking CLFE into consideration, Van Vechten and Martin calculated the optical spectrum of diamond within RPA.[18] They found that the inclusion of CLFE shifted the spectral weight in the imaginary part of the dielectric function ϵ_2 to higher energies in comparison to the calculation without CLFE, a result that worsens the agreement with the experiment. Hanke and Sham investigated the role of CLFE in diamond using a time-dependent Hartree-Fock approximation in a Wannier representation[1]. They also found that CLFE within the RPA shift the spectral weight in the optical spectrum of diamond to higher energies. However, the additional inclusion of the electron-hole attraction reverses this trend and shifts spectral weight in ϵ_2 back to lower energies. Thus the combined treatment of RPA local-field and excitonic effects improves the agreement with experiment.[19] Just recently these results have been confirmed by an *ab initio* calculation with the detailed inclusion of the electron-hole interaction.[10] In silicon, where the electron wave functions are not as localized as in diamond, a similar behavior of the local-field effects was found, although the effects were not as strong as in diamond.[4,10,11]

Although CLFE cannot be neglected in the optical limit, an increasing strength of CLFE is expected with increasing momentum transfer which samples more localized excitations.[13] Simultaneously, the loss function loses its collective character and is dominated more and more by single-particle excitations. To our knowledge, there are no measurements of the $\mathbf{q}$-dependent loss function of single-crystalline diamond up to now. In this paper, we present the loss function of diamond measured along the high-symmetry directions over a wide range of momentum transfers and energy

PRB <u>61</u> 10 149

loss. We found the plasmon dispersion to be considerably anisotropic with a strong interplay between the plasmon excitation and interband transitions in the energy range of the plasmon energy. By comparing the experimentally determined loss function with *ab initio* local-density approximation (LDA) calculations under inclusion or neglect of CLFE, we will show that the CLFE are most pronounced in the $\langle 100 \rangle$ crystal direction and for larger momentum transfers. This is also what one expects from the crystal structure as the distance between two carbon atoms in the $\langle 100 \rangle$ direction is longer than those in the $\langle 111 \rangle$ and $\langle 110 \rangle$ directions. Significant differences between our calculations and our experiments that still remain, demonstrate the extent of many-particle effects (XCLFE), that contribute to the loss function but are treated only insufficiently in our calculations.

II. EXPERIMENT

The EELS measurements were performed at room temperature using a purpose-built spectrometer[20] with a primary electron energy of 170 keV. The energy and momentum resolution was chosen to be 160 meV and 0.06 Å^{-1}, respectively. As sample we have used a natural diamond single-crystal type IIa. For the EELS in transmission measurements we have prepared free standing thin films of 100 nm thickness by Ar-ion beam milling. Electron diffraction enables us to orient the single-crystal *in situ* with respect to a selected crystal direction. The diffraction spectra clearly showed the sharp bragg peaks that are expected for a single crystal.

III. *Ab initio* CALCULATION OF THE LOSS FUNCTION

For the theoretical description the bandstructure was obtained from a self-consistent *ab initio* pseudopotential calcu-

lation within LDA carried out in the plane-wave basis with a large cut-off of 50 Rydbergs. Norm-conserving pseudopotentials of carbon were used. From the LDA band structure the loss function has been calculated. It is defined as

$$W(\mathbf{q}, \omega) = - \text{Im}[\epsilon^{-1}(\mathbf{q}, \omega)_{\mathbf{G}=0, \mathbf{G}'=0}], \quad (1)$$

where ϵ^{-1} is the inverse of the already introduced dielectric matrix. It can be represented as follows:

$$\epsilon^{-1} = 1 + v_c \chi^{(0)} [1 - (v_c + f_{xc}) \chi^{(0)}]^{-1}. \quad (2)$$

Here, all objects are matrices with respect to $\mathbf{G}, \mathbf{G}'$, the reciprocal lattice vectors. $\chi^{(0)}(\mathbf{q}, \omega)_{\mathbf{G}, \mathbf{G}'}$ denotes the density response of the noninteracting electrons in the Kohn-Sham scheme, $v_c = 4\pi/|\mathbf{q} + \mathbf{G}|^2 \delta_{\mathbf{G}, \mathbf{G}'}$ is the Coulomb interaction in Fourier space and f_{xc} describes exchange and correlation effects.[21] Within the adiabatic LDA approximation, f_{xc} is ω independent and given by

$$f_{xc}(\mathbf{q}, \omega)_{\mathbf{G}, \mathbf{G}'} = f_{xc}(\mathbf{G}' - \mathbf{G})$$

$$= \int d^3 r e^{i(\mathbf{G}' - \mathbf{G})\mathbf{r}} \frac{dV_{XC}(\mathbf{r})}{dn(\mathbf{r}')} \delta(\mathbf{r} - \mathbf{r}'), \quad (3)$$

where $V_{XC}(\mathbf{r})$ and $n(\mathbf{r}')$ are the self-consistent Kohn-Sham potential of the system and its electron density, respectively.

The response matrices, whose size was about 60, depending on the momentum transfer, have been calculated integrating over a dense mesh of 16384 **k** points in the Brillouin zone. In the following, we denote the calculations with the full matrix form of Eqs. (2), i.e., including CLFE, as ''LDA-full.'' ''LDA-dia'' describes the calculations, where the ma-
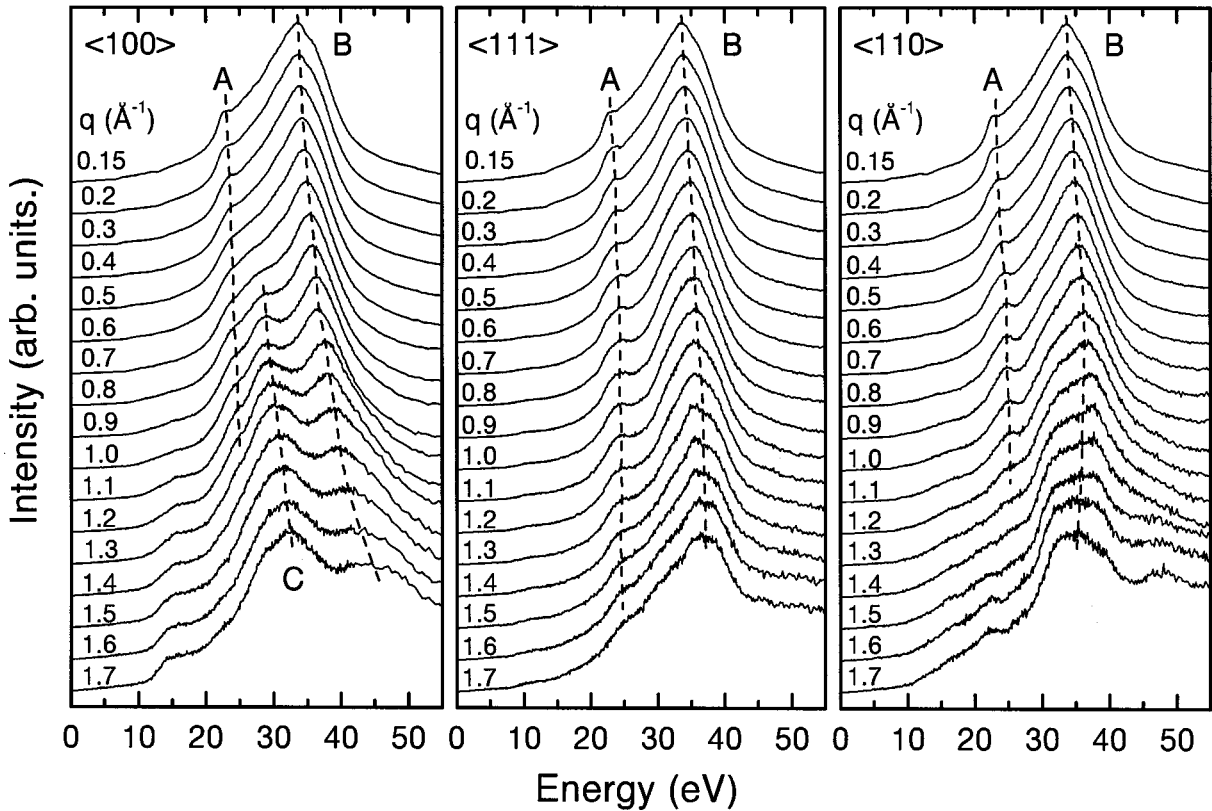

FIG. 1. Experimental loss functions for various momentum transfers along the $\langle 100 \rangle$, $\langle 111 \rangle$, and $\langle 110 \rangle$ crystal directions. The dashed lines elucidate the dispersion of the most prominent peaks as a guide to the eye.
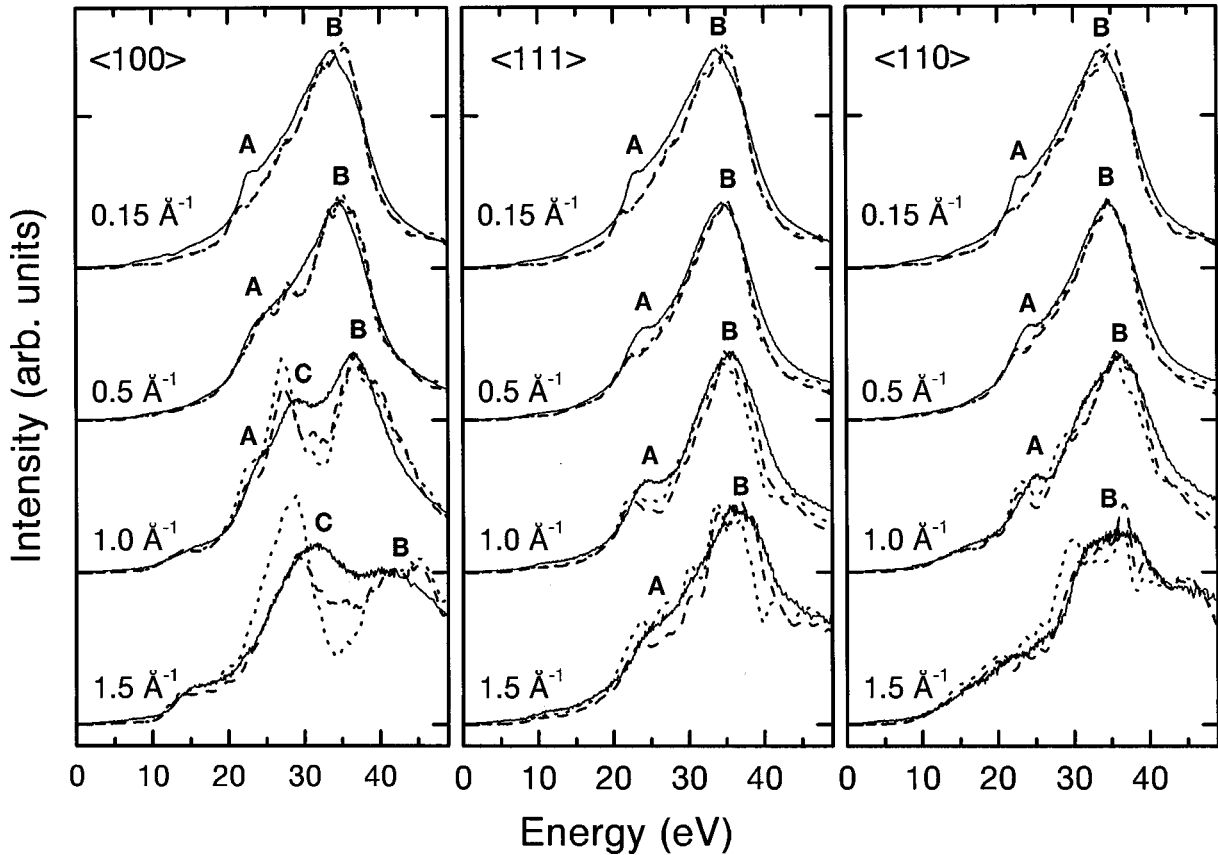
FIG. 2. Comparison of experimental loss functions (solid lines) with LDA calculations that include LFE (LDA-full, dashed lines) or neglect LFE (LDA-dia, dotted lines). Shown are spectra for some chosen momentum transfers along the $\langle 100 \rangle$, $\langle 111 \rangle$, and $\langle 110 \rangle$ crystal directions.

trix form of Eq. (2) has been neglected and with this the CLFE. The neglect of f_{xc} leads to the RPA response function. By considering both, the imaginary and the real parts of the dielectric function in the LDA-full calculation, we can determine the connection between the single-particle excitation spectrum and the visible features in the loss function.

IV. RESULTS AND DISCUSSION

Figure 1 presents EELS measurements for the $\langle 100 \rangle$, $\langle 111 \rangle$, and $\langle 110 \rangle$ directions with different momentum transfers, starting with 0.15 Å^{-1} up to 1.7 Å^{-1}. The spectra are corrected for the elastic line and multiple scattering[20] and are normalized to the plasmon intensity. The most prominent peaks in the spectra are labeled A, B, and C. The dashed lines elucidate the dispersion of the respective peaks. In Fig. 2, we present the calculated loss functions, with the inclusion (LDA-full) and without the inclusion (LDA-dia) of CLFE, in comparison to the experimental loss functions for some chosen momentum transfers. Additionally, Figs. 3 and 4 display LDA-full calculations of the real (ϵ_1) and the imaginary (ϵ_2) part of the dielectric function for several momentum transfers along the $\langle 100 \rangle$ (Fig. 3), the $\langle 111 \rangle$ (Fig. 4), and the $\langle 110 \rangle$ (Fig. 4) directions. The position of the peaks A, B, and C that are visible in the loss spectra are marked with dashed lines.

The main feature in Fig. 1 (peak B) in all spectra is the volume plasmon of diamond, visible near 33 eV in the limit of small momentum transfer q. The large electron density of

diamond is responsible for the relatively high plasmon energy. Striking at a first glance are the large halfwidth and the asymmetry of the plasmon peak.[22] The most significant feature which renders the plasmon peak asymmetric is the peak labeled A near 23 eV. In all directions and for $q = 0.15$ and 0.5 Å^{-1}, peak A is clearly visible. As surface plasmons decrease much more rapidly than volume plasmons with increasing wave vector q, peak A can be attributed to interband transitions. The LDA calculations of the loss function (Fig. 2), where no surface losses are included, as well as the ϵ_2 spectra (Fig. 3) also show clearly a peak near 23 eV.

At small momentum transfers, the loss spectra for all crystal directions look quite similar. This is to be expected for a cubic crystal near the optical limit. This changes if we enlarge the momentum transfer, where the anisotropy of the band structure becomes important. At 0.5 Å^{-1}, the peak A has nearly vanished in the $\langle 100 \rangle$ direction whereas it is still clearly visible in the other directions. Quite striking is the appearance of peak C in Fig. 1 near 0.8 Å^{-1} in the $\langle 100 \rangle$ direction. This peak disperses to higher energies and becomes stronger in intensity with increasing momentum transfer. Simultaneously, peak B shows a large dispersion, much larger than in the other directions. The reason for this behavior can be seen in Fig. 3: ϵ_2 for $q = 1.0$ and 1.5 Å^{-1} shows large interband transitions near 33 and 38 eV and local minima in ϵ_1 near 35 and 40 eV, respectively, in addition to the zero crossings of ϵ_1 near 27 eV. This causes two maxima in the loss function, which represents a coupled system of a
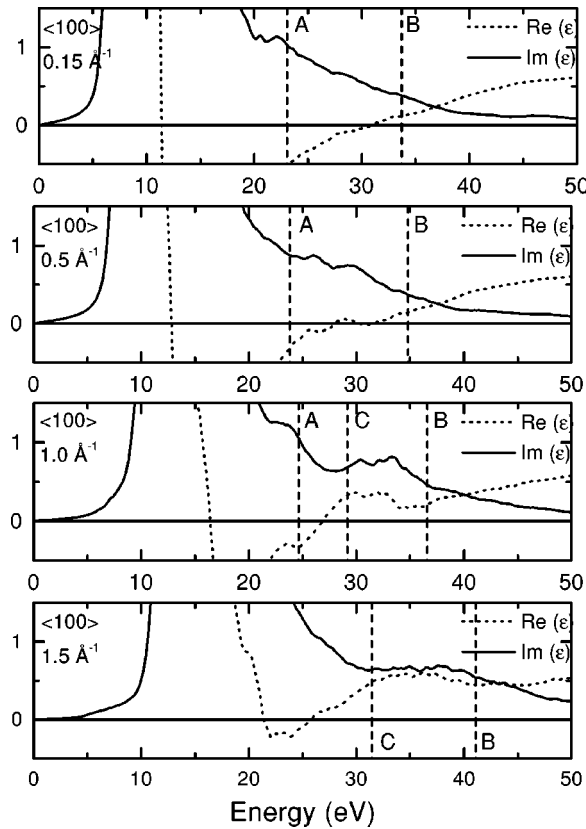
FIG. 3. Calculated real parts (ϵ_1, dotted lines) and imaginary parts (ϵ_2, solid lines) of ϵ for some selected momentum transfers along the $\langle 100 \rangle$ direction. The position of the peaks A, B, and C that are visible in the loss functions are marked with dashed lines.

FIG. 4. Calculated real parts (ϵ_1, dotted lines) and imaginary parts (ϵ_2, solid lines) of ϵ for some selected momentum transfers along the $\langle 111 \rangle$ and the $\langle 110 \rangle$ directions. The position of the peaks A, B, and C that are visible in the loss functions are marked with dashed lines.

plasmon excitation and interband transitions.

In comparison to the $\langle 100 \rangle$ direction, the plasmon dispersion in the $\langle 111 \rangle$ and the $\langle 110 \rangle$ directions is much less pronounced. Up to a momentum transfer of 0.7 Å^{-1} the plasmon dispersion is almost the same for all crystal directions. Above 0.8 Å^{-1}, where peak C appears in the $\langle 100 \rangle$ direction, the plasmon peaks in the $\langle 111 \rangle$ and the $\langle 110 \rangle$ directions nearly keeping their original shape up to $q = 1.7$ Å^{-1}. Nevertheless the LDA calculations in Fig. 2 and also the corresponding ϵ_1 and ϵ_2 spectra (Fig. 4) indicate, that the plasmon-like peak in the loss function experiences also a coupling between a collective plasmon excitation and interband transitions in the energy range of the plasmon energy.

The impact of CLFE is evident from Fig. 2, where we show a comparison of the LDA-full and the LDA-dia calculations. As we have already discussed, one expects that CLFE become stronger with increasing momentum transfers and that this effect should at first appear in the $\langle 100 \rangle$ direction. Figure 2 shows that this is indeed the case. For $q = 0.15$ and 0.5 Å^{-1}, there is hardly an influence of CLFE. For 1.0 Å^{-1} one sees small contributions in the $\langle 111 \rangle$ and the $\langle 110 \rangle$ directions but a pronounced influence of CLFE in the $\langle 100 \rangle$ direction. Considering the calculated loss functions with q = 1.5 Å^{-1}, CLFE are clearly visible for all crystal directions. Especially in the $\langle 100 \rangle$ direction the effect is very large. At $q = 1.5$ Å^{-1} it is also evident that the inclusion of CLFE shifts spectral weight to higher energies, which significantly improves the agreement with the experiment. In calculations of the imaginary part of the dielectric function in
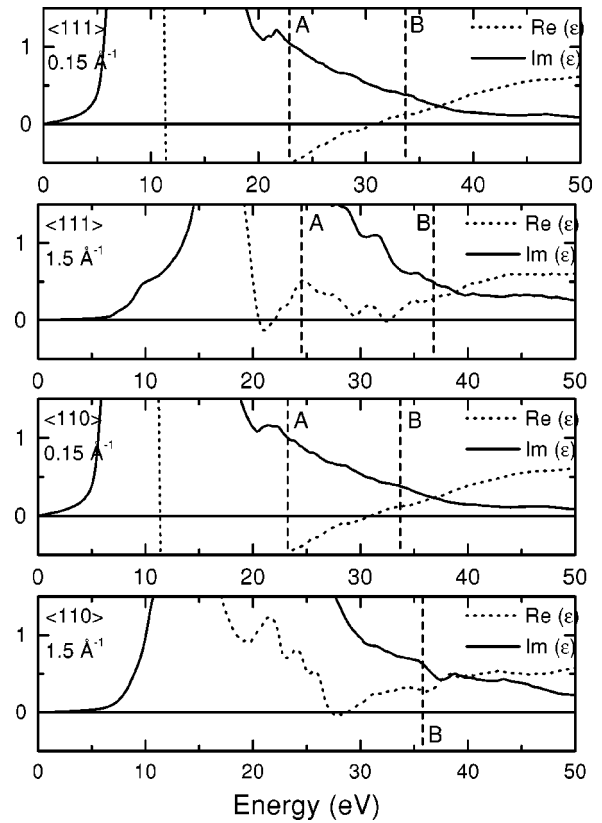
the optical limit for diamond, a shift of spectral weight to higher energies with the inclusion of local-field effects has also been found.[1,18] At a first glance, it appears rather strange that CLFE modify ϵ_2 noticeable but not the loss function, in the limit of small momentum transfers. However, this is a consequence of the fact that the local environment influences strongly the single-particle excitations that determine ϵ_2. On the other hand, the plasmon excitation is a density oscillation dominated by the long range part of the Coulomb interaction where a large number of electrons (and thus electron-hole excitations) collectively participate. There is a further observation that is likely to be connected to this point: if one considers the loss functions for 1.0 and 1.5 Å^{-1} momentum transfers in the $\langle 100 \rangle$ direction, it is striking that CLFE are mainly visible at the position of peak C but not at peak B. The explanation could again be a different character of the excitations that cause the peaks: peak C is dominated by single-particle excitations whereas peak B has a more collective character, dominated by the plasmon excitation, and therefore is more independent of CLFE.

The influence of the bandstructure, the CLFE and the XCLFE as well as the interplay between the different effects on the plasmon dispersion were investigated for a large quantity of materials. For example in NiO a large influence of CLFE on the loss function was expected because the system is very inhomogeneous. But it has been shown that the influence of CLFE in this system is related to the existence of certain interband transitions that are different for the loss

function and the static screening. Resulting from this it has been found that CLFE are important for the static screening but not for the loss function in NiO.[26] Also the alkali metals and especially Cs were the objects of wide interest. The negative plasmon dispersion of Cs that was found experimentally,[27] was mainly explained by bandstructure effects caused by the $3d$ electrons. But also CLFE that are strongly enhanced by the localized core electrons are of considerable influence.[28] Additionally it was found that also XCLFE that are interrelated with the CLFE play an important role.[29] The importance of electron correlations has been expected because of the low-electron density in Cs. Diamond in contrast has a large electron density and therefore electron correlations are expected to be of minor influence.

Concerning our investigations we can ascertain that the main experimental trends are clearly reproduced by the theory, nevertheless there still remain significant differences between experiment and the calculations. On the one hand, these differences originate from the well-known underestimation of the energy gaps by the LDA approximation. On the other hand, exchange and correlation effects (such as excitonic contributions) seem not to be negligible in the response. This was already shown in the optical limit by Hanke and Sham[1] and more recently by Benedict *et al.*[10] We note that the consideration of f_{xc}, which describes the exchange and correlation corrections in our calculations of the response function within LDA, does not significantly improve the agreement with experiment, as can be seen from a comparison of the calculations with (Fig. 2) and without (not shown) the inclusion of f_{xc}. Thus, a complete understanding of the dielectric response of diamond requires a more sophisticated treatment of exchange and correlation effects.

V. SUMMARY

In conclusion, we have shown that the dielectric response of diamond, probed with EELS in transmission, shows a large anisotropy with higher momentum transfers. By a comparison with LDA calculations we attribute this anisotropy to the interaction between the collective plasmon excitation and interband transitions in the energy range of the plasmon energy. We found that with increasing momentum transfers crystal local-field effects contribute more and more strongly to the loss function with the latter changing its character from more collective to more single-particle like. Still remaining deviations between experiment and calculations point to the importance of many-particle effects, in particular, excitonic effects that are insufficiently treated in our calculations.

ACKNOWLEDGMENTS

[1] W. Hanke and L. J. Sham, Phys. Rev. Lett. **33**, 582 (1974); Phys. Rev. B **12**, 4501 (1975).

[2] K. Sturm, Adv. Phys. **31**, 1 (1982).

[3] S. G. Louie, J. R. Chelikowsky, and M. L. Cohen, Phys. Rev. Lett. **34**, 155 (1975).

[4] W. Hanke and L. J. Sham, Phys. Rev. B **21**, 4656 (1980); G. Strinati, H. J. Mattausch, and W. Hanke, *ibid.* **25**, 2867 (1982).

[5] M. Hybertsen and S. G. Louie, Phys. Rev. Lett. **55**, 1418 (1985); Phys. Rev. B **34**, 5390 (1986); **35**, 5602 (1987).

[6] R. W. Godby, M. Schlüter, and L. J. Sham, Phys. Rev. B **37**, 10 159 (1988).

[7] M. Rohlfing, P. Krüger, and J. Pollmann, Phys. Rev. B **48**, 17 791 (1993).

[8] V. I. Gavrilenko and F. Bechstedt, Phys. Rev. B **54**, 13 416 (1996).

[9] F. Bechstedt, K. Tenelsen, B. Adolph, and R. Del Sole, Phys. Rev. Lett. **78**, 1528 (1997).

[10] L. X. Benedict, E. L. Shirley, and R. B. Bohn, Phys. Rev. B **57**, R9385 (1998).

[11] S. Albrecht, L. Reining, R. Del Sole, and G. Onida, Phys. Rev. Lett. **80**, 4510 (1998).

[12] M. Rohlfing and S. G. Louie, Phys. Rev. Lett. **81**, 2312 (1998).

[13] S. R. Nagel and T. A. Witten, Jr., Phys. Rev. B **11**, 1623 (1975).

[14] P. Nozières and D. Pines, Phys. Rev. **109**, 741 (1958).

[15] H. Ehrenreich and M. H. Cohen, Phys. Rev. **115**, 786 (1959).

[16] S. Adler, Phys. Rev. **126**, 413 (1962).

[17] N. Wiser, Phys. Rev. **129**, 62 (1963).

[18] J. A. Van Vechten and R. M. Martin, Phys. Rev. Lett. **28**, 446 (1972).

[19] R. A. Roberts and W. C. Walker, Phys. Rev. **161**, 730 (1967).

[20] J. Fink, Adv. Electron. Electron Phys. **75**, 121 (1989).

[21] E. K. U. Gross and W. Kohn, Adv. Quantum Chem. **21**, 255 (1990).

[22] A strongly asymmetric shape of the plasmon excitation has also been observed for, e.g., CdTe (Ref. 23) and Zn (Ref. 24). But in this case localized d-states that are absent in diamond cause interband transitions near the plasmon energy. Diamond rather has to be compared with silicon where one finds an almost symmetric plasmon peak with a much smaller halfwidth (Ref. 25). This is an expression of the much more free electron like band structure of silicon in comparison to diamond.

[23] H. Dröge, A. Fleszar, W. Hanke, M. Sing, M. Knupfer, J. Fink, F. Groschenhofer, C. R. Becker, R. Kargenbauer, and H. P. Steinrück, Phys. Rev. B **59**, 5544 (1999).

[24] K. Widder, M. Knupfer, O. Knauff, and J. Fink, Phys. Rev. B **56**, 10 154 (1997).

[25] J. Stiebling and H. Raether, Phys. Rev. Lett. **40**, 1293 (1978).

[26] F. Aryasetiawan, O. Gunnarsson, M. Knupfer, and J. Fink, Phys. Rev. B **50**, 7311 (1994).

[27] A. vom Felde, J. Fink, T. Büche, B. Scheerer, and N. Nücker, Europhys. Lett. **4**, 1037 (1987); A. vom Felde, J. Sprösser-Prou, and J. Fink, Phys. Rev. B **40**, 10 181 (1989).

[28] F. Aryasetiawan and K. Karlsson, Phys. Rev. Lett. **73**, 1679 (1994).

[29] A. Fleszar, R. Stumpf, and A. G. Eguiluz, Phys. Rev. B **55**, 2068 (1997).